

Melonjosephite, calcium iron hydroxy phosphate: its crystal structure

ANTHONY R. KAMPF¹ AND PAUL B. MOORE

Department of the Geophysical Sciences

The University of Chicago

Chicago, Illinois 60637

Abstract

Melonjosephite, $\text{Ca}_2[(\text{Fe}_{0.5}^{2+}\text{Fe}_{0.5}^{3+})_4(\text{OH})_2(\text{PO}_4)_4]$, $Z = 2$, orthorhombic, $a = 9.542(1)$, $b = 10.834(1)$, $c = 6.374(1)\text{\AA}$, space group $Pbam$, has chains of edge-sharing Fe–O octahedra oriented parallel to the c axis. $R(hkl) = 0.043$ for 728 independent reflections. Dimers of edge-sharing Fe–O octahedra share vertices with octahedra of the chains to form sheets parallel to $\{010\}$ with the formula $[\text{Fe}_2(\text{OH})(\text{O}_p)_7]$.² The (PO_4) tetrahedra link within and between sheets to form a framework structure. The CaO_7 polyhedron occurs in pockets between the sheets.

Although two independent Fe atom sites occur in the structure, the mixed valence pair (Fe^{2+} , Fe^{3+}) is evenly distributed between them. Average bond distances are $\text{Ca–O} = 2.47\text{\AA}$, $\text{Fe}(1)\text{–O} = 2.08\text{\AA}$, $\text{Fe}(2)\text{–O} = 2.06\text{\AA}$, $\text{P}(1)\text{–O} = 1.54\text{\AA}$, $\text{P}(2)\text{–O} = 1.54\text{\AA}$.

Regions of the melonjosephite crystal structure can be directly related to the octahedral tetramer found in leucophosphate, $\text{K}_2[\text{Fe}_4^{3+}(\text{OH})_2(\text{H}_2\text{O})_2(\text{PO}_4)_4] \cdot 2\text{H}_2\text{O}$, and regions of the structure of olmsteadite, $\text{K}_2\text{Fe}_2^{2+}[\text{Fe}_2^{2+}\text{Nb}_2^{5+}\text{O}_4(\text{H}_2\text{O})_4(\text{PO}_4)_4]$ and related compounds.

Introduction

Melonjosephite is a recent discovery, described by Franolet (1973) as black fibrous masses which replace a member of the alluaudite group from the Angarf-Sud pegmatite, Anti-Atlas, Morocco. Owing to its dark color, the presence of mixed valences of iron, and unique cell criteria, we have investigated its detailed structure.

Experimental section

Dr. A.-M. Franolet kindly provided fragments of the type material. It was obvious that difficulty would be encountered in obtaining a suitable single crystal; indeed, a space group could not be determined in the original study owing to inferior quality of the single crystals. Repeated splitting of the fibers, however, yielded an individual grain measuring $0.06\text{ mm} (\parallel a) \times 0.06\text{ mm} (\parallel b) \times 0.12\text{ mm} (\parallel c)$ suitable for study. Despite the small size of the crystal, the material afforded sharp reflections which presented no difficulty in data collection.

The crystal was mounted with its c axis parallel to the spindle, and 1688 reflections were gathered on a Picker FACS-1 automated diffractometer utilizing graphite monochromatized $\text{MoK}\alpha$ radiation, $2\theta_{\text{max}} = 55^\circ$, scan speed 2° min^{-1} , with 20-second stationary background measurements on each side of the peak. Owing to low mosaic spread, a half-angle scan width of only 0.7° was required.

Absorption correction was not applied owing to the relatively low linear absorption coefficient ($\mu = 57.4\text{ cm}^{-1}$), the small size of the crystal, and its approximately cylindrical shape. During reduction of the data to obtain $|F_o|$ symmetry equivalent reflections were averaged. After correction for Lorentz and polarization effects and excluding the systematic extinctions, 728 independent reflections were available for further analysis.

Least-squares refinement of 30 reference reflections measured on the automated diffractometer yielded $a = 9.542(1)$, $b = 10.834(1)$, and $c = 6.374(1)\text{\AA}$, in good agreement with the earlier study of Franolet. In addition, the systematic absences suggested space groups $Pbam$ or $Pba2$. The success of the crystal structure analysis is submitted as evidence to support the centrosymmetric group $Pbam$. A calculated powder pattern based on the coordinates of the structure

¹ Present address: Geology–Mineralogy Section, Los Angeles County Museum of Natural History, 900 Exposition Boulevard, Los Angeles, California 90007.

² O_p = phosphate oxygen

Table 1. Calculated and observed powder data for melonjosephite

Calculated			Observed*		Calculated			Observed*	
I/Io	d(calc)	hkl	I/Io	d(obs)	I/Io	d(calc)	hkl	I/Io	d(obs)
9	7.161	110	15	7.15	5	1.801	422		
20	6.374	001	10	6.37	4	1.791	350	5	1.794
52	5.417	020	90	5.42	8	1.761	152	5	1.763
15	4.771	200	20	4.76	4	1.732	521		
10	4.711	120	15	4.70	20	1.710	233	15	1.711
29	3.788	121	20	3.787	4	1.709	161		
27	3.602	211	25	3.597	4	1.677	252	5	1.679
12	3.580	220	25	3.580	7	1.647	143	5	1.648
9	3.378	130	15	3.380	3	1.632	261		
50	3.187	002	30	3.185	2	1.631	531	5	1.632
11	3.122	221	15	3.121	12	1.619	512	5	1.621
100	3.052	310	100	3.049	20	1.594	004	10	1.594
5	2.984	131	5	2.984	2	1.590	600		
67	2.912	112	40	2.912	1	1.587	333	10	1.590
20	2.879	230	25	2.881	4	1.587	403		
6	2.747	022	10	2.749	7	1.571	062	15	1.571
47	2.709	040	90	2.710	7	1.570	413		
29	2.650	202	10	2.647	5	1.561	352		
53	2.624	231	60	2.624	6	1.561	442	10	1.563
6	2.412	141	5	2.411	7	1.560	540		
9	2.387	330			8	1.555	451	15	1.558
40	2.381	222	30	2.383	4	1.528	170		
4	2.204	312			16	1.526	620	20	1.525
34	2.188	411	35	2.187	4	1.523	423	10	1.521
13	2.113	150	20	2.114	10	1.492	262	15	1.493
5	2.065	421			5	1.491	532	10	1.490
4	2.063	042			2	1.441	134	10	1.441
12	2.037	113	10	2.036	4	1.440	460	10	1.437
9	2.006	151	10	2.007	7	1.434	271	5	1.434
5	1.990	430	10	1.990	7	1.413	314	5	1.414
16	1.973	250	30	1.974	2	1.376	622		
4	1.941	203			4	1.376	063	5	1.378
7	1.937	123	5	1.938	7	1.373	044	10	1.374
19	1.910	402	10	1.909	4	1.373	523	10	1.372
10	1.894	242	10	1.896					

*Fransolet (1973).

analysis is compared with the data of Fransolet in Table 1.

Solution and refinement of the structure

The chemical analysis [Fransolet (1973)] indicated a rather simple composition, with only minor amounts of substituents entering into the ideal formula. The weight percents of components for the ideal formula $\text{CaFe}^{2+}\text{Fe}^{3+}(\text{OH})(\text{PO}_4)_2$ are given in parentheses: P_2O_5 39.96(39.47) percent; Al_2O_3 0.17, Fe_2O_3 21.81(22.26); MgO 1.18, Li_2O 0.07, FeO 17.39(20.03); MnO 0.44, Na_2O 0.48, CaO 14.99(15.63); H_2O^+ 2.50(2.51); insol. 0.97; $\Sigma = 99.96$ (100.00) percent.

A three-dimensional Patterson synthesis, $P(uvw)$, was prepared. At this stage, an obvious relationship to the known structures of montgomeryite, vauxite, and olmsteadite was noted, and it was possible to

Table 2. Atomic coordinate and isotropic thermal vibration parameters for melonjosephite*

	x	y	z	B(\AA^2)
Fe(1)	0	0	0.2670(1)	0.66(2)
Fe(2)	0.3434(1)	0.0553(1)	$\frac{1}{2}$	0.58(2)
Ca	0.4259(2)	0.2324(1)	0	0.96(3)
P(1)	0.0921(2)	0.2441(2)	$\frac{1}{2}$	0.44(3)
O(1)	0.0285(3)	0.1826(3)	0.3028(5)	0.57(6)
O(2)	0.2511(5)	0.2307(4)	$\frac{1}{2}$	0.86(8)
O(3)	0.0502(5)	0.3817(4)	$\frac{1}{2}$	0.75(8)
P(2)	0.2081(2)	0.4779(2)	0	0.48(3)
O(4)	0.3730(5)	0.4691(4)	0	0.90(9)
O(5)	0.3392(4)	0.0566(3)	0.1866(5)	0.74(6)
O(6)	0.1563(5)	0.3466(4)	0	0.98(9)
OH	0.3474(5)	0.4725(4)	$\frac{1}{2}$	0.78(8)
H	0.320	0.400	$\frac{1}{2}$	

* Estimated standard errors in parentheses refer to the last digit. The hydrogen atom was located on a difference synthesis and was not refined.

Table 4. Polyhedral interatomic distances and angles for melonjosephite*

Fe(1)			Ca			
2 Fe	-O(1)	2.010(3) Å	2 Ca	-O(1) ⁽²⁾	2.352(3)	
2	- OH ⁽²⁾	2.101(4)	1	-O(6) ⁽²⁾	2.360(5)	
2	-O(4) ⁽²⁾	2.116(3)	2	-O(5)	2.393(4)	
average		2.076 Å	1	-O(4)	2.613(5)	
			1	-O(6)	2.854(5)	
			average		2.474	
			P(1)			
1 O(4) ⁽²⁾ -O(4) ⁽³⁾		2.514(10) [†]	72.9(2) [°]	1 P(1)	-O(2)	1.525(5)
2 O(1) - OH ⁽²⁾		2.718(5)	82.7(2)	1	-O(3)	1.543(5)
2 O(1) - OH ⁽³⁾		2.857(5)	88.0(2)	2	-O(1)	1.547(3)
2 O(1) -O(4) ⁽²⁾		2.937(5)	90.7(2)	average		1.541
1 OH ⁽²⁾ - OH ⁽³⁾		2.972(10) [†]	90.0(2)			
2 O(1) -O(4) ⁽³⁾		3.156(5)	99.8(2)			
2 O(4) ⁽²⁾ - OH ⁽²⁾		3.197(1)	98.6(1)			
average		2.935	90.2 [°]			
Fe(2)			2 O(1) -O(3)	2.505(5)	108.3(2)	
2 Fe(2)	-O(5)	1.998(3)	1 O(1) -O(1) ⁽¹⁾	2.513(6)	108.7(3)	
1	- OH ⁽³⁾	2.030(5)	1 O(2) -O(3)	2.521(7)	110.5(3)	
1	-O(3) ⁽³⁾	2.088(5)	2 O(1) -O(2)	2.523(5)	110.4(2)	
1	-O(2)	2.094(5)	average	2.515	109.4	
1	-O(3) ⁽²⁾	2.137(5)				
average		2.058	P(2)			
			1 P(2)	-O(6)	1.506(5)	
			2	-O(5) ⁽³⁾	1.532(3)	
			1	-O(4)	1.577(5)	
			average		1.537	
1 O(3) ⁽²⁾ -O(3) ⁽³⁾		2.737(10) [†]	80.7(2)	1 O(5) ⁽³⁾ -O(5) ⁽⁵⁾	2.379(6)	101.9(3)
2 O(5) - OH ⁽³⁾		2.827(5)	89.2(1)	1 O(4) -O(6)	2.457(7)	105.7(3)
2 O(5) -O(2)		2.872(5)	89.1(1)	2 O(5) ⁽³⁾ -O(4)	2.533(5)	109.2(2)
2 O(5) -O(3) ⁽²⁾		2.913(5)	90.9(1)	2 O(5) ⁽³⁾ -O(6)	2.568(5)	115.4(2)
2 O(5) -O(3) ⁽³⁾		2.949(5)	90.9(1)	average	2.506	109.5
1 OH ⁽³⁾ -O(2)		2.951(7)	91.3(2)			
1 O(3) ⁽³⁾ - OH ⁽³⁾		3.002(7)	92.1(2)			
1 O(2) -O(3) ⁽²⁾		3.102(7)	95.7(2)			
average		2.910	90.0			
Hydrogen Bond						
OH...O(2)		2.776(6) Å				

* Equivalent positions referred to Table 1 are listed as superscripts and are: 1 = x, y, -z; 2 = $\frac{1}{2}x$, $\frac{1}{2}y$, z; 3 = $\frac{1}{2}x$, $\frac{1}{2}y$, -z; 4 = -x, -y, z; 5 = $\frac{1}{2}x$, $\frac{1}{2}y$, z.

[†] Fe-Fe shared edge.

unambiguously derive all interatomic distance vectors based on a local cluster model common to all these structures (Fig. 4). From this model, the remaining nonhydrogen atoms could be located from a γ' -general synthesis (Ramachandran and Srinivasan, 1970).

Full-matrix least-squares refinement of the atomic coordinate parameters and isotropic thermal vibration parameters led to rapid convergence to $R = 0.043$ and $R_w = 0.034$, where $R = \sum ||F_o| - |F_c|| / \sum |F_o|$ and $R_w = [\sum w(|F_o| - |F_c|)^2 / \sum w F_o^2]^{1/2}$ for all 728 independent F_o . We employed a highly modified version of the familiar ORFLS program of Busing *et al.* (1962), and scattering curves for Ca^{2+} , $(\text{Fe}^{3+} + \text{Fe}^{2+})/2$, P^0 and O^{1-} from Cromer and Mann (1968).

The final cycle minimized $\sum w ||F_o| - |F_c||^2$ where $w = \sigma_{F-2}$. A total of 39 parameters were varied, with a data to variable parameter ratio of about 20:1. The secondary extinction coefficient (Zachariasen, 1968) is $c_o = 2.1(3) \times 10^{-6}$. Table 2 lists the atomic coordinate and isotropic thermal vibration parameters, Table 3 the structure factors,³ and Table 4 the polyhedral interatomic distances and angles.

The hydrogen atom was located in a final difference Fourier synthesis. Four residuals were of greater

³ To obtain a copy of this table, order Document AM-76-036 from the Business Office, Mineralogical Society of America, 1909 K Street, N.W., Washington, D.C. 20006. Please remit \$1.00 in advance for the microfiche.

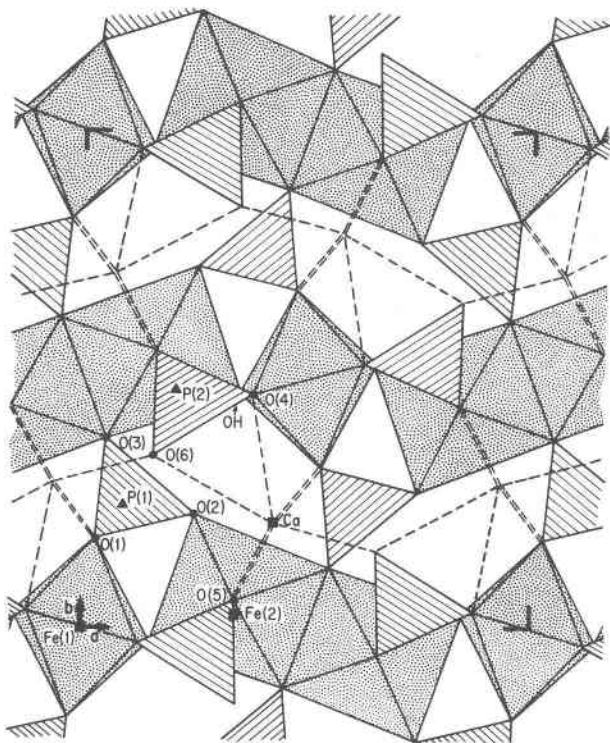


Fig. 1. Polyhedral diagram of the melonjosephite crystal structure down [001]. The octahedra are stippled, the tetrahedra are ruled and the Ca-O bonds appear as dashed spokes.

magnitude, but three of these were close to the Ca atom, which we suspect exhibits some anisotropy.

Description of the structure

Melonjosephite possesses a structure which is new, although regions of its arrangement can be readily characterized on the basis of already known and classified structures of other phosphate species. Figure 1 is a polyhedral diagram projected down the [001] direction and Figure 2 a projection down [010]. The most prominent feature is a linear edge-sharing $\frac{1}{2}[\text{Fe}(1)(\text{O}_P)_2(\text{OH})_2]$ octahedral chain parallel to the *c* axis (Fig. 2). Symmetry equivalent chains are cross-linked along the *a* axis by edge-sharing dimers of composition $\text{Fe}(2)_2(\text{OH})_2(\text{O}_P)_6$. These dimers join at their opposing vertices to the chain via the (OH) ligand. Thus, (OH) links three Fe-O octahedra together at a common vertex. A rather open octahedral sheet is formed parallel to {010} possessing the formula $[\text{Fe}_2(\text{OH})(\text{O}_P)_7]$. The (PO_4) tetrahedra link within and between the sheets to form a framework structure, and the CaO_7 polyhedra occur in pockets between the sheets. Owing to a rather even distribution of bonds, there is no obvious cleavage direction;

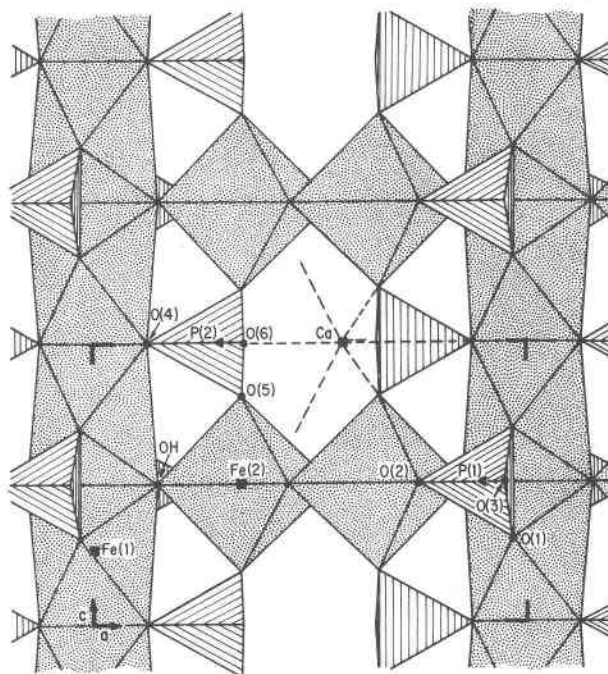


Fig. 2. Polyhedral diagram of the melonjosephite crystal structure down [010]. Note the octahedral edge-sharing chains which parallel to [001].

indeed, Fransolet (1973) reports a possible cleavage transverse to the fiber axis, *c*, but expresses some doubt about its existence.

At first the structure was quite new to us, until discrete regions were recognized which could be immediately compared with other structures. Figure 3

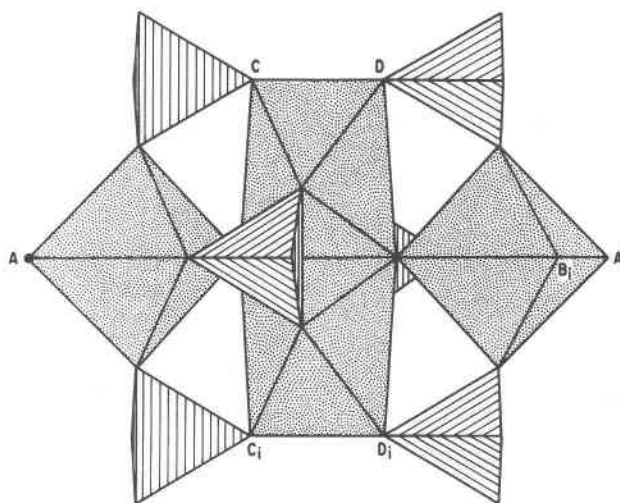


Fig. 3. The cluster of composition $[\text{Fe}_4(\text{OH})_2(\text{PO}_4)_6(\text{O}_P)_4]$ which can be discerned in Fig. 2. This cluster also appears in the crystal structure of leucophosphate although the two structures differ in condensation at points A, Ai, Bi, C, Ci, D, and Di.

shows a fragment of composition $[\text{Fe}_4(\text{OH})_2(\text{PO}_4)_6(\text{O}_P)_4]$, cut out from Figure 2. The local geometry of this cluster is identical with that found in leucophosphite, $\text{K}_2[\text{Fe}_4^{3+}(\text{OH})_2(\text{H}_2\text{O})_2(\text{PO}_4)_4] \cdot 2\text{H}_2\text{O}$, the structure of which was described by Moore (1972). Amarantite, $[\text{Fe}_4\text{O}_2(\text{H}_2\text{O})_8(\text{SO}_4)_4] \cdot 6\text{H}_2\text{O}$, also possesses the same octahedral tetramer although the order and ratios of ligands are different (Süsse, 1968). In leucophosphite, the links at A and A_i in Figure 3 are to (PO_4) tetrahedra; in melonjosephite, these link to the octahedral chains. B_i and its inversion equivalent are water molecules in leucophosphite; in melonjosephite, these link to (PO_4) tetrahedra. The points C and C_i , and D and D_i do not link further in leucophosphite; in melonjosephite, these link to equivalent clusters forming octahedral edge-sharing chains. The geometry of the octahedral tetramer and the six linked tetrahedra are preserved to a remarkable degree in both structures, and it doubtless represents an arrangement whose character is electrostatically favorable. Such a cluster is expected to play a potentially significant role in other as yet undescribed structures.

Nor is that all! Looking at Figure 1, it is seen that another cluster can be distinguished which shares geometrical properties with another structural family. In Figure 4, it is seen that this cluster has composition $[\text{Fe}_3(\text{OH})_2(\text{PO}_4)_4(\text{O}_P)_6]$. Further octahedral corner-sharing at B and B_2 leads to the chain structures documented in olmsteadite, $\text{K}_2\text{Fe}_2^{2+}[\text{Fe}_2^{2+}\text{Nb}_2^{5+}\text{O}_4(\text{H}_2\text{O})_4(\text{PO}_4)_4]$ (Moore *et al.*, 1976); and schoonerite $\text{Zn}_2\text{Mn}_2^{2+}\text{Fe}_2^{2+}(\text{H}_2\text{O})_{14}[\text{Fe}_2^{2+}\text{Fe}_2^{3+}(\text{OH})_4(\text{PO}_4)_6]$

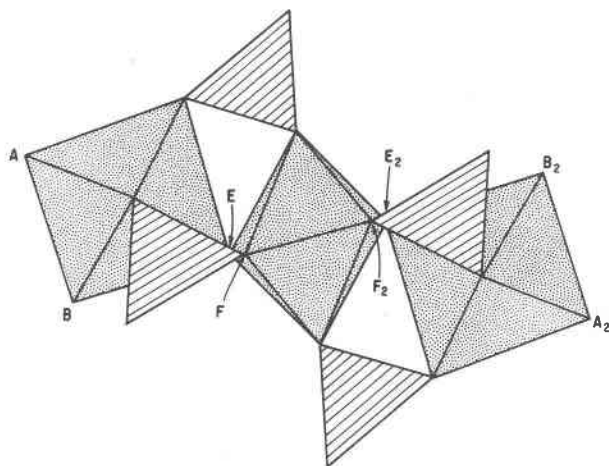


Fig. 4. The cluster of composition $[\text{Fe}_3(\text{OH})_2(\text{PO}_4)_4(\text{O}_P)_6]$ which can be discerned in Fig. 1. This cluster is the basis for other 6.4\AA repeat structures such as olmsteadite, schoonerite, montgomeryite, and vauxite. Note that by switching E and F , a *trans*-arrangement can be obtained with respect to the central octahedron.

$\cdot 4\text{H}_2\text{O}$ (Moore and Kampf, 1977; Kampf, 1977). If E and F are reversed, a *trans*-arrangement ensues: this is found in the chain structures of montgomeryite, $\text{Ca}_4\text{Mg}(\text{H}_2\text{O})_{12}[\text{Al}_4(\text{OH})_4(\text{PO}_4)_6]$, and vauxite, $\text{Fe}_2^{2+}(\text{H}_2\text{O})_4[\text{Al}_4(\text{OH})_4(\text{H}_2\text{O})_4(\text{PO}_4)_4] \cdot 4\text{H}_2\text{O}$ (Moore and Araki, 1974).

Thus, melonjosephite can be conceived as a hybrid structure, intermediate to leucophosphite and the chain structures mentioned above. As more structures of basic ferrous-ferric phosphates come to light, a pattern seems to be emerging: the great diversity of species is based on relatively few kinds of clusters and the variety of ways in which these clusters can link to each other, including the manifold ligand isomerisms about these clusters, thus accounting for the unusual richness of species. To better convey the relationship of melonjosephite with the other structures, we express the formula as $\text{Ca}_2[(\text{Fe}_{0.5}^{2+}\text{Fe}_{0.5}^{3+})_4(\text{OH})_2(\text{PO}_4)_4]$, of which there are two such formula units in the cell.

Bond distances and angles

The bond distances and angles are summarized in Table 4. The Fe-O averages are $\text{Fe}(1)\text{-O} = 2.08\text{\AA}$ and $\text{Fe}(2)\text{-O} = 2.06\text{\AA}$. These distances are approximately between $\text{Fe}^{2+}\text{-O} = 2.12\text{-}2.17\text{\AA}$ and $\text{Fe}^{3+}\text{-O} = 1.98\text{-}2.02\text{\AA}$ averages reported for other ferrous and ferric phosphate crystal structures and agree very well for the average $\text{Fe}(1)\text{-O} = \text{Fe}_{0.5}^{2+}\text{Fe}_{0.5}^{3+}\text{-O} = 2.07\text{\AA}$ and $\text{Fe}(2)\text{-O} = \text{Fe}_{0.5}^{2+}\text{Fe}_{0.5}^{3+}\text{-O} = 2.06\text{\AA}$ obtained from the tables of Shannon and Prewitt (1969). The numbers in brackets before the oxygens are the average coordination numbers. There is little doubt that melonjosephite is a true mixed-valence compound with Fe^{2+} and Fe^{3+} evenly distributed over the two available sites.

The distances between $\text{Fe}(1)$ positions along the edge-sharing chains are 2.97\AA and 3.40\AA . Owing to mixed-valences, homonuclear valence transfer absorption effects are expected to be very strong along this direction. Indeed, Franolet (1973) reported $X = c$ (deep brown, nearly opaque). In addition, $Y = a$ (greenish-brown), and this direction receives most of the $\text{Fe}(2)\text{-Fe}(2')$ component across the shared edge in the dimer. The remaining direction, $Z = b$ (yellow-gold, somewhat greenish) is devoid of direct Fe-Fe' links other than through (PO_4) tetrahedral vertices, and receives only the relatively weak $\text{Fe}(2)\text{-Fe}(2')$ component.

One curious feature in the structure appears in the $\text{O}(4)^{(2)}\text{-O}(4)^{(3)} = 2.51\text{\AA}$ shared edge and the $\text{OH}^{(2)}\text{-OH}^{(3)} = 2.97\text{\AA}$ shared edge belonging to the octahedral chain (the superscripts refer to equivalent

Table 5. Electrostatic bond strength–bond length relationships in melonjosephite*

	Ca	Fe(1)	Fe(2)	P(1)	P(2)	H _d	H _a	Δp_x	Ca	Fe(1)	Fe(2)	P(1)	P(2)
O(1)	1	1		1				-0.05	-0.12	-0.07		<i>+0.01</i>	
O(2)			1	1			1	-0.17			<i>+0.04</i>	-0.02	
O(3)			2	1				+0.08			<i>+0.03,</i> <i>+0.09</i>	<i>+0.00</i>	
O(4)	1	2			1			+0.37	+0.14	<i>+0.04,</i> <i>+0.04</i>			+0.04
O(5)	1		1		1			-0.05	-0.08		-0.06		+0.00
O(6)	2				1			-0.18	-0.11, <i>+0.38</i>				-0.03
OH		2	1			1		+0.08		<i>+0.03,</i> <i>+0.03</i>	<i>-0.03</i>		

* The number of cations bonded to anions are listed. The deviation from electrostatic neutrality, Δp_x , is given. Deviations in bond distances, Δd , from polyhedral averages are listed. Those Δd which are opposite in sign to Δp_x are italicized.

positions listed in Table 4). The latter edge can be referred to the O(9)–O(9)' = 2.60Å edge in amarantite and the O(9)–O(9)' = 3.01Å edge in leucophosphate, since in all three structures the tetrameric arrangement is conserved. It is noted that this edge distance more closely resembles that of leucophosphate, since in both structures an (OH)⁻ anion links to the three octahedra. In amarantite, an *oxo*-anion bridges the three iron atoms, resulting in extreme anion electrostatic under-saturation by cations ($\Delta p_x = -0.50$) and subsequent foreshortening of the Fe–O distances. The short O(4)⁽²⁾–O(4)⁽³⁾ edge, on the other hand, results from repulsion of the Fe–Fe cations away from that edge.

The hydrogen atom was located on the difference synthesis and its position is compatible with an inferred OH...O(2) = 2.78Å bond. This bond is also consistent with the electrostatic bond strength sums determined in the following section. The calcium atom resides in an open pocket in the structure, most easily seen in Figure 2. It exhibits five short distances (Ca–O = 2.35 – 2.39Å) and two long distances [O(4) = 2.61Å and O(6) = 2.85Å], and is geometrically an octahedron with a split vertex. This split pair corresponds to an edge of the P(2)O₄ tetrahedron, doubtless contributing to the long bonds owing to Ca–P(2) repulsion.

Electrostatic valence balances

Table 5 lists the valence bond strengths for the oxygen atoms in melonjosephite on the basis of the number and kinds of cations coordinating to them. A bond strength of $s = 5/6$ is ascribed to the hydrogen donor (H_d), and $s = 1/6$ for the hydrogen acceptor

(H_a) as suggested by Baur (1970) on empirical grounds. A deviation, Δp_x , from neutrality is then compared with a deviation, Δd , in the individual bond distance from the polyhedral average.

It is seen that four contradictions occur in Table 5, since Δp_x and Δd are of opposite sign. Three of these, however, are small deviations from the polyhedral average and are offset by deviations of the same sign in the same row. Only Ca–O(6) possesses a serious contradiction although it is compensated by the remaining bonds. O(4), with $\Delta p_x = +0.37$, deviates most seriously from local electrostatic neutrality and accordingly exhibits all four bonds longer than average.

Acknowledgments

We are grateful to Dr. André-Marie Fransolet for single crystal material from the type specimen and to Dr. Takaharu Araki for assistance in the structure analysis.

This study was supported by the NSF grant GA 40543 (Geochemistry Section) and through the Materials Research Laboratory grant administered to The University of Chicago.

References

- Baur, W. H. (1970) Bond-length variation and distorted coordination polyhedra in inorganic crystals. *Trans. Am. Crystallogr. Assoc.*, 6, 129–155.
- Busing, W. A., K. O. Martin and H. A. Levy (1962) ORFLS, a Fortran crystallographic least-squares program. *U.S. Natl. Tech. Inf. Serv. ORNL-TM-305*.
- Cromer, D. T. and J. B. Mann (1968) X-ray scattering factors computed from numerical Hartree-Fock wave-functions. *Acta Crystallogr.*, A24, 321–324.
- Fransolet, A.-M. (1973) La mélonjosephite, CaFe²⁺Fe³⁺(PO₄)₂(OH), une nouvelle espèce minérale. *Bull. Soc. fr. Mineral. Cristallogr.*, 96, 135–142.

- Kampf, A. R. (1977) Schoonerite, its atomic arrangement. *Am. Mineral.*, 62, in press.
- Moore, P. B. (1972) Octahedral tetramer in the crystal structure of leucophosphate. *Am. Mineral.*, 57, 397-410.
- and T. Araki (1974) Montgomeryite, its crystal structure and relation to vauxite. *Am. Mineral.*, 59, 843-850.
- , ——, A. R. Kampf and I. M. Steele (1976) Olmsteadite, $K_2Fe_2^{2+}[Fe_2^{2+}(Nb,Ta)_2^{5+}O_4(H_2O)_4(PO_4)_4]$, a new species, its crystal structure and relation to vauxite and montgomeryite. *Am. Mineral.*, 61, 5-11.
- Moore, P. B. and A. R. Kampf (1977) Schoonerite: a new species. *Am. Mineral.*, 62, in press.
- Ramachandran, G. N. and R. Srinivasan (1970) *Fourier Methods in Crystallography*. Wiley-Interscience, New York, 96-119.
- Shannon, R. D. and C. T. Prewitt (1969) Effective ionic radii in oxides and fluorides. *Acta Crystallogr.*, B25, 925-946.
- Süsse, P. (1968) The crystal structure of amarantite, $Fe_2(SO_4)_2O \cdot 7H_2O$. *Z. Kristallogr.*, 127, 261-275.
- Zachariasen, W. H. (1968) Experimental tests of the general formula for the integrated intensity of a real crystal. *Acta Crystallogr.*, A24, 212-214.

*Manuscript received, May 21, 1976; accepted
for publication, July 27, 1976.*